CHEMISTRY OF MATERIALS
Article

Chem. Mater. **2010,** *22,* 3995–4006 3995
DOI:10.1021/cm1007075

Synthesis and Optical Properties of a Rod−Coil Diblock Copolymer with Polyoxometalate Clusters Covalently Attached to the Coil Block

Sanjiban Chakraborty,[†] Andrew Keightley,[‡] Vladimir Dusevich,[§] Yong Wang,[§] and Zhonghua Peng*,[†]

[†]*Department of Chemistry,* [‡]*School of Biological Sciences, and* [§]*Department of Oral Biology, University of Missouri-Kansas City, Kansas City, Missouri 64110*

Received March 10, 2010. Revised Manuscript Received June 4, 2010

A rod−coil diblock copolymer (DCP) containing an oligo(phenylene vinylene) (OPV) rigid block and a polystyryl-type flexible block with polyoxometalate (POM) clusters as side chain pendants has been successfully synthesized. The coil block of 2,6-dimethyl-4-vinyl aniline protected by phthalic anhydride was prepared by atom transfer radical polymerization (ATRP). The terminal bromo-end group was then converted to an azide which subsequently coupled with an ethynyl terminated OPV rod block by "click" chemistry. After removing the phthalimide protection groups in the coil block to give free aryl amines, POM clusters were finally attached to the coil block covalently to yield the first POM-containing DCP. The hybrid DCP shows two absorption bands, one at 370 nm which is attributed to the ligand-to-metal charge transfer transition associated with imido-functionalized POM clusters, and the other at 450 nm which is due to the $\pi-\pi^*$ transition of the OPV backbone. Cyclic voltammetry measurements show a distinct reversible reduction process at −1.1 eV, significantly cathodically shifted compared to that of free hexamolybdate cluster. These results indicate that the POM clusters are indeed covalently linked to the DCP. Although little fluorescence quenching is observed in solution, the POM cluster is found to quench 74% of the OPV fluorescence in films. Such a significant fluorescence quenching is likely due to a photoinduced electron-transfer process from the OPV donor to the POM cluster, making it a potential candidate as an efficient photovoltaic material. Preliminary film morphology studies show that the hybrid DCP aggregates very differently from its precursor DCPs.

Introduction

Diblock copolymers (DCPs) are perhaps the most extensively studied polymer architectures in the past couple of decades not only because of their unlimited combinations of different blocks with compositional and structural variations but also because of their often superior materials properties resulting from the realization of the desired phase-separated morphologies.[1] While all organic DCPs continue to dominate the field, organic−inorganic hybrid DCPs have drawn increasing attention.[2] In particular,

*To whom correspondence should be addressed. E-mail: pengz@umkc.edu.

(1) (a) Helfand, E.; Wasserman, Z. R. In *Developments in Block Copolymers-1*; Goodman, I.; Ed.; Applied Science Publishers: New York, 1982; Chapter 4. (b) Bates, F. S.; Fredrickson, G. H. *Annu. Rev. Phys. Chem.* **1990**, *41*, 525. (c) Bates, F. S. *Science* **1991**, *251*, 898. (d) Stalmach, U.; de Boer, B.; Videlot, C.; van Hutten, P. F.; Hadziioannou, G. *J. Am. Chem. Soc.* **2000**, *122*, 5464. (e) Whitesides, G. M.; Grzybowski, B. *Science* **2002**, *295*, 2418.(f) Hamley, I. W. *The Physics of Block Copolymers*; Oxford University Press, Inc.: New York, 1998. (g) Hadjichristidis, N.; Pitsikalis, M.; Iatrou, H *Adv. Polym. Sci.* **2005**, *189*, 1. (h) Fredrickson, G. H.; Bates, F. S. *Annu. Rev. Mater. Sci.* **1996**, *26*, 501. (i) Floudas, G.; Vazaiou, B.; Schipper, F.; Ulrich, R.; Wiesner, U.; Iatrou, H.; Hadjichristidis, N. *Macromolecules* **2001**, *34*, 2947. (j) Khandpur, A. K.; Foerster, S.; Bates, F. S.; Hamley, I. W.; Ryan, A. J.; Bras, W.; Almdal, K.; Mortensen, K. *Macromolecules* **1995**, *28*, 8796. (k) Matsen, M. W.; Bates, F. S. *Macromolecules* **1996**, *29*, 1091. (l) Simon, P. F. W.; Ulrich, R.; Spiess, H. W.; Wiesner, U. *Chem. Mater.* **2001**, *13*, 3464. (m) Choucair, A.; Eisenberg, A. *Eur. Phys. J. E* **2003**, *10*, 37. (n) Stewart, S.; Liu, G. *Angew. Chem., Int. Ed.* **2000**, *39*, 340. (o) Jain, S.; Bates, F. S. *Science* **2003**, *300*, 460. (p) Li, Z.; Kesselman, E.; Talmon, Y.; Hillmyer, M. A.; Lodge, T. P. *Science* **2004**, *306*, 98. (q) Pochan, D. J.; Chen, Z. Y.; Cui, H. G.; Hales, K.; Qi, K.; Wooley, K. L. *Science* **2004**, *306*, 94. (r) Spatz, J. P.; Moessmer, S.; Moller, M. *Angew. Chem., Int. Ed. Engl.* **1996**, *35*, 1510. (s) Lodge, T. P.; Muthukumar, M. *J. Phys. Chem.* **1996**, *100*, 13275. (t) Stupp, S. I.; LeBonheur, V.; Walker, K.; Li, L. S.; Huggins, K. E.; Keser, M.; Amstutz, A. *Science* **1997**, *276*, 384.

(2) (a) Ribot, F.; Banse, F.; Sanchez, C.; Lahcini, M.; Jousseaume, B. *J. Sol-Gel Sci. Technol.* **1997**, *8*, 529. (b) Foerster, S.; Antonietti, M. *Adv. Mater.* **1998**, *10*, 195. (c) Watson, K. J.; Zhu, J.; Nguyen, S. T.; Mirkin, C. A. *J. Am. Chem. Soc.* **1999**, *121*, 462. (d) Okumura, A.; Tsutsumi, K.; Hashimoto, T. *Polym. J.* **2000**, *32*, 520. (e) Pyun, J.; Matyjaszewski, K.; Kowalewski, T.; Savin, D.; Patterson, G.; Kickelbick, G.; Huesing, N. *J. Am. Chem. Soc.* **2001**, *123*, 9445–9446. (f) Matsuura, Y.; Matsukawa, K.; Kawabata, R.; Higashi, N.; Niwa, M.; Inoue, H. *Polymer* **2002**, *43*, 1549. (g) Gratt, J. A.; Cohen, R. E. *J. Appl. Polym. Sci.* **2004**, *88*, 177. (h) Koh, K.; Ohno, K.; Tsujii, Y.; Fukuda, T. *Angew. Chem., Int. Ed.* **2003**, *42*, 4194. (i) Laruelle, G.; Parvole, J.; Francois, J.; Billon, L. *Polymer* **2004**, *45*, 5013. (j) Ro, H. W.; Kim, K. J.; Theato, P.; Gidley, D. W.; Yoon, D. Y. *Macromolecules* **2005**, *38*, 1031. (k) Chen, Y.; Du, J.; Xiong, M.; Zhang, K.; Zhu, H. *Macromol. Rapid Commun.* **2006**, *27*, 741. (l) Stone, D. A.; Allcock, H. A. *Macromolecules* **2006**, *39*, 4935. (m) Zhou, J.; Wang, L.; Dong, X.; Chen, T.; Yang, Q.; Chen, C.; Chen, X. *Nanotechnology* **2006**, *17*, 2745. (n) Zhang, L.; Abbenhuis, H. C. L.; Yang, Q.; Wang, Y. M.; Magusin, P. C. C. M.; Mezari, B.; Van Santen, R. A.; Li, C. *Angew. Chem., Int. Ed.* **2007**, *46*, 5003. (o) Masuda, T.; Yamamoto, S.; Moriya, O.; Kashio, M.; Sugizaki, T. *Polym. J.* **2008**, *40*, 126. (p) Hirai, T.; Leolukman, M.; Hayakawa, T.; Kakimoto, M.; Gopalan, P. *Macromolecules* **2008**, *41*, 4558. (q) Liao, C. C.; Wu, H. Y.; Saikia, D.; Pan, Y. C.; Chen, Y. K.; Fey, G. T. K.; Kao, H. M. *Macromolecules* **2008**, *41*, 8956. (r) Zhang, K.; Gao, L.; Chen, Y. *Macromolecules* **2008**, *41*, 1800. (s) Zhang, W.; Zhuang, X.; Li, X.; Lin, Y.; Bai, J.; Chen, Y. *React. Funct. Polym.* **2009**, *69*, 124. (t) Monge, S.; Zhang, X.; Giani, O.; Robin, J. J. *React. Funct. Polym.* **2009**, *69*, 380.

Published on Web 06/15/2010

metal-containing DCPs have been actively pursued in recent years. For example, Manners has studied a variety of DCPs with one block containing ferrocenes.[3] Chan,[4] Schubert,[5] and others[6] have explored DCPs containing transition metal complexes. While these studies are exemplary, they include only discrete metal centers; block copolymers containing metal clusters, as far as we know, have not yet been reported. Among various metal−oxygen clusters, polyoxometalates (POM) are most attractive not only because of their structural versatility and rich optoelectronic properties but also because of their discrete molecule structures which allow surface functionalization in a controlled and rational way.[7] Indeed, a number of POM-containing organic−inorganic hybrids have recently been reported,[8−26] among which a few examples involve POM-containing polymers.[27] While most POM-containing polymers are based on an insulating polymer backbone, we have previously reported both main chain and side chain POM-containing conjugated polymers and have demonstrated that POM clusters as electron acceptors, in conjunction with organic π-conjugated segments as electron donors, may find applications as novel photovoltaic (PV) materials.[28] The PV performances of our reported hybrid conjugated polymers are, however, not spectacular. This is not surprising though as an efficient PV device requires not only efficient photoinduced charge transfer but also efficient and separate charge transporting pathways for positive and negative charge carriers. A conjugated polymer with POM clusters uniformly distributed either in the main chain or in side chains may exhibit efficient photoinduced charge separation, but possess no separate charge transporting channels for electrons and holes. Since electrons transport through hopping among POM clusters while holes transport through aggregated conjugated segments, a polymer system which can segregate the two structural components may be able to provide the separate domains for different charge transport. With these considerations in mind, we have set out to synthesize a rod−coil DCP with POM clusters linked to the coil block. The rod block is a conjugated polymer which serves as the electron donor, while the POM cluster in the coil block acts as the electron acceptor. If bicontinuous phase separated domains can be formed through DCP self-assembly, such a hybrid DCP may possess significantly improved PV performance over our previously reported hybrid conjugated polymers. In this paper, we report the synthesis and optical properties of the first such POM-containing hybrid DCP.

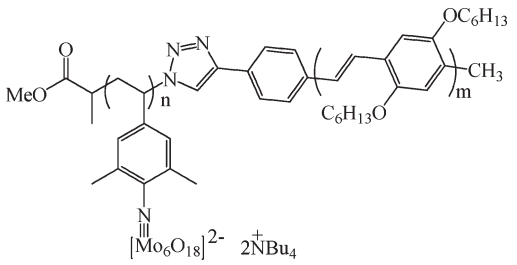

Figure 1. Structure of a hybrid rod−coil diblock copolymer.

Results and Discussion

Synthesis. Figure 1 shows the structure of the POM-containing DCP. Poly(phenylene vinylene) or PPV is used

(3) (a) Manners, I. *Chem. Commun*. **1999**, *10*, 857. (b) Manners, I. *Science* **2001**, *294*, 1664. (c) Wang, X.; Winnik, M. A.; Manners, I. *Macromolecules* **2005**, *38*, 1928.
(4) (a) Hou, S.; Man, K. Y.; Chan, W. K. *Langmuir* **2003**, *19*, 2485. (b) Cheng, K. W.; Chan, W. K. *Langmuir* **2005**, *21*, 5247.
(5) Gohy, J. F.; Lohmeijer, B. G. G.; Varshney, S. K.; Schubert, U. S. *Macromolecules* **2002**, *35*, 7427.
(6) Lammertink, R. G. H.; Hempenius, M. A.; Thomas, E. L.; Vancso, G. J. J. *Polym. Sci. Part B: Polym. Phys*. **1999**, *37*, 1009.
(7) (a) Pope, M. T. *Heteropoly and Isopoly Oxometalates*; Springer-Verlag: New York, 1983. (b) Pope, M. T.; Muller, A. *Angew. Chem., Int. Ed. Engl*. **1991**, *30*, 34. (c) *Polyoxometalates: From Platonic Solids to Anti-Retroviral Activity*;Pope, M. T., Muller, A., Eds.; Kluwer Academic Publishers: Dordrecht, The Netherlands, 1994. (d) Hill, C. L., guest editor; Chem. Rev. **1998**, *98*, No. 1. (e) Gouzerh, P.; Proust, A. *Chem. Rev*. **1998**, *98*, 77.
(8) (a) Shimidzu, T.; Ohtani, A.; Aiba, M.; Honda, K. *J. Chem. Soc., Faraday Trans*. **1988**, *84*, 3941. (b) Bidan, G.; Genies, E. M.; Lapkowski, M. *J. Chem. Soc., Chem. Commun*. **1988**, 533. (c) Fabre, B.; Bidan, G.; Laplowski, M. *J. Chem. Soc., Chem. Commun*. **1994**, 1509. (d) Gomez-Romero, P.; Lira-Cantu, M. *Adv. Mater*. **1997**, *9*, 144. (e) Otero, T, F.; Cheng, S. A.; Huerta, C. F. *J. Phys. Chem. B*. **2000**, *104*, 10522. (f) Otero, T, F.; Cheng, S. A.; Alonso, D.; Huerta, F. *J. Phys. Chem. B*. **2000**, *104*, 10528. (g) Cheng, S. A.; Otero, T. F.; Coronado, E.; Gomez-Garcia, C. J.; Martinez-Ferrero, E.; Gimenez-Saiz, C. *J. Phys. Chem. B* **2002**, *106*, 7585.
(9) Liu, S.; Kurth, D. G.; Bredenkotter, B.; Volkmer, D. *J. Am. Chem. Soc*. **2002**, *124*, 12279.
(10) Judeinstein, P. *Chem. Mater*. **1992**, *4*, 4.
(11) Mayer, C. R.; Thouvenot, R.; Lalot, T. *Chem. Mater*. **2000**, *12*, 257.
(12) (a) Schroden, R. C.; Blanford, C. F.; Melde, B. J.; Johnson, B. J. S.; Stein, A. *Chem. Mater*. **2001**, *13*, 1074. (b) Johnson, B. J. S.; Stein, A. *Inorg. Chem*. **2001**, *40*, 801.
(13) Moore, A. R.; Kwen, H.; Beatty, A. M.; Maatta, E. A. *Chem. Commun*. **2000**, *18*, 1793.
(14) Favette, S.; Hasenknopf, B.; Vaissermann, J.; Gouzerh, P.; Roux, C. *Chem. Commun*. **2003**, *21*, 2664.
(15) Schubert, U. *Chem. Mater*. **2001**, *13*, 3487.
(16) Sanchez, C.; de A. A. Soler-Illia, G. J.; Ribot, F.; Lalot, T.; Mayer, C. R.; Cabuil, V. *Chem. Mater*. **2001**, *13*, 3061.
(17) Reinoso, S.; Vitoria, P.; Felices, L. S.; Lezama, L.; Gutierrez-Zorrilla, J. M. *Chem.—Eur. J*. **2005**, *11*, 1538.
(18) Zhu, Y.; Xiao, Z.; Ge, N.; Wang, N.; Wei, Y.; Wang, Y. *Cryst. Growth Des*. **2006**, *6*, 1620.
(19) Szreder, T.; Wishart, J. F.; Dietz, M. L. *J. Phys. Chem. B* **2007**, *111*, 4685.
(20) Poulos, A. S.; Constantin, D.; Davidson, P.; Imperor, M.; Pansu, B.; Panine, P.; Nicole, L.; Sanchez, C. *Langmuir* **2008**, *24*, 6285.
(21) Zhang, J.; Song, Y. F.; Cronin, L.; Liu, T. *J. Am. Chem. Soc*. **2008**, *130*, 14408.
(22) Cao, R. G.; Liu, S. X.; Liu, Y.; Tang, Q.; Wang, L.; Xie, L. H.; Su, Z. M. *J. Solid State Chem*. **2009**, *182*, 49.
(23) (a) Zhu, L.; Zhu, Y.; Meng, X.; Hao, J.; Li, Q.; Wei, Y.; Lin, Y. *Chem.—Eur. J*. **2008**, *14*, 10923. (b) Zhu, Y.; Wang, L.; Hao, J.; Xiao, Z.; Wei, Y.; Wang, Y. *Cryst. Growth Des*. **2009**, *9*, 3509. (c) Zhu, Y.; Wang, L.; Hao, J.; Yin, P.; Zhang, J.; Li, Q.; Zhu, L.; Wei, Y. *Chem.—Eur. J*. **2009**, *15*, 3076.
(24) Compain, J. D.; Mialane, P.; Dolbecq, A.; Marrot, J.; Proust, A.; Nakatani, K.; Yu, P.; Secheresse, F. S. *Inorg. Chem*. **2009**, *48*, 6222.
(25) Tian, A. X.; Ying, J.; Peng, J.; Sha, J. Q.; Su, Z. M.; Pang, H. J.; Zhang, P. P.; Chen, Y.; Zhu, M.; Shen, Y. *Cryst. Growth Des*. **2010**, *10*, 1104.
(26) Wang, Y.; Li, W.; Wu, L. *Langmuir* **2009**, *25*, 13194.
(27) (a) Adamczyk, L.; Kulesza, P. J.; Miecznikowski, K.; Palys, B.; Chojak, M.; Krawczyk, D. *J. Electrochem. Soc*. **2005**, *152*, E98. (b) Chen, H.; Xie, L.; Lu, H.; Yang, Y. *J. Mater. Chem*. **2007**, *17*, 1258. (c) Han, Y.; Xiao, Y.; Zhang, Z.; Liu, B.; Zheng, P.; He, S.; Wang, W. *Macromolecules* **2009**, *42*, 6543. (d) Qi, W.; Wu, L. *Polym. Int*. **2009**, *58*, 1217. (e) Kulak, A.; Kokorin, A.; Kulak, T.; Meissner, D. *Proc. Est. Acad. Sci*. **2009**, *58*, 12. (f) Schaming, D.; Allain, C.; Farha, R.; Goldmann, M.; Lobstein, S.; Giraudeau, A.; Hasenknopf, B.; Ruhlmann, L. *Langmuir* **2010**, *26*, 5101.
(28) (a) Meng, L.; Xie, B.; Kang, J. H.; Chen, T.; Yang, Y.; Peng, Z. *Chem. Mater*. **2005**, *17*, 402. (b) Xu, B.; Lu, M.; Kang, J.; Wang, G.; Brown, J.; Peng, Z. *Chem. Mater*. **2005**, *17*, 2841.

Scheme 1. Synthesis of an Azide Terminated PS Block

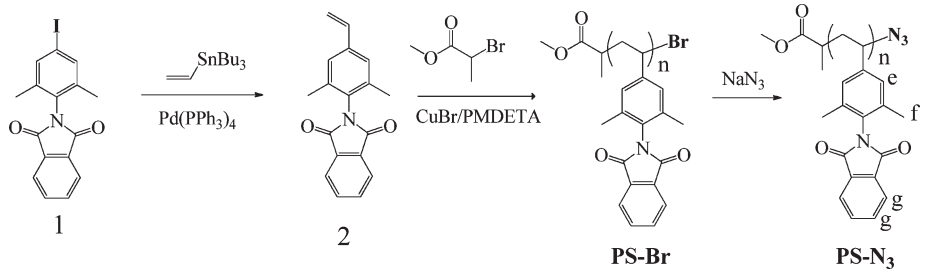

as the rod block which is attached to the coil block through the triazole functional group whereas the hexamolybdate cluster is connected to the coil block via an imido linkage. The hexamolybdate cluster has a molecular formula of $[Mo_6O_{19}]^{2-}$ with tetrabutylammonium as the counterion.

Polymer hybrids can be realized, in principle, by two different pathways: the post-polymerization hybridization approach and the post-hybridization polymerization (hybridization first) approach. The first route involves the synthesis of a precursor DCP with functional pendants on one block followed by the covalent linkage of the POM cluster. The second route initiates from the synthesis of hybrid monomers, which are in turn used directly for polymerization. Both avenues while enjoying some advantages, at the same time are inflicted with some drawbacks. The former approach has better control over the degree of polymerization of each block with the flexibility of synthesizing polymer hybrids with varying clusters. There may be, however, a lack of control over the extent of cluster attachment. The latter approach, while ensuring complete cluster functionalization on the coil block, demands the development of new chemistry: the living polymerization of POM containing monomers has yet to be demonstrated though living polymerization of styrene monomer using trivanadium substituted polytungstate type POM initiator has been reported.[27c] While we have made efforts on both fronts concomitantly and our preliminary results indicate that vinyl functionalized POM clusters can indeed undergo polymerization under ATRP conditions, this paper instead will focus on the first route, that is, the post-polymerization hybridization pathway to prepare our targeted hybrid DCP. In other words, a DCP with pendant free aryl amine is synthesized first, followed by cluster attachment to yield the targeted hybrid.

To prepare the rod−coil DCP, we set to synthesize an azide terminated coil block and an ethynyl functionalized PPV block. The two blocks can then be joined together through "click" chemistry. Scheme 1 shows the synthesis of the coil block. Compound **1** was prepared by iodinating 2,6-dimethylaniline according to a literature procedure,[29] followed by protection of the free amine group by phthalic anhydride. Stille coupling reaction of **1** with tributyl vinyltin gave the vinyl monomer **2** in 60% yield. Monomer **2** was then subjected to atom transfer radical polymerization (ATRP).[30] With CuBr, *N*,*N*,*N*,*N*,*N*-pentamethyldiethylenetriamine (PMDETA) and methyl-2-bromopropionate (MBP) as the catalyst, ligand and initiator, respectively, monomer **2** was polymerized to form the flexible coil block. It is noted that in the course of the reaction, active chain ends with the bromo group could gradually convert to dead chains, possibly by the elimination of bromine because of chain transfer to the aliphatic amine ligand[31] or by the β-H elimination reaction.[32] To ensure that all chain ends are active, the ATRP of **2** was quenched prior to complete monomer-to-polymer conversion. The bromo-end functional group of the coil block obtained by ATRP was then converted to an azide group by nucleophilic substitution reaction with sodium azide.[33]

The ^{1}H NMR spectra of monomer **2**, **PS-Br** and **PS-N$_3$** are shown in Figure 2. One observes that after polymerization, the vinyl protons of monomer **2**, observed at 5.27, 5.75, and 6.67 ppm, completely disappeared, while new broad signals around 1.7 and 2.2 ppm corresponding to methylene protons in the polymer backbone appeared. Three broad aromatic signals are observed at 6.65, 7.71, and 7.80 ppm, among which the first can be assigned to aromatic protons in the bridging phenyl ring (proton e in Scheme 1) while the other two are attributed to protons of the phthalimide unit (proton g). The dominant alkyl signal at 2.03 ppm is assigned to the two phenyl-bonding methyl groups.

End groups give small but clear signals. The initiating end gives methoxy signals at 3.42 ppm, and methyl signals (signal b) around 0.9 ppm. Signals corresponding to the propagating end are not as clear. If one expands the region with chemical shifts from 4.0 to 5.0 ppm, one sees a clear signal around 4.43 ppm which can be assigned to the proton associated with the Br-bonding carbon. After converting to an azide, this signal is shifted to 3.95 ppm. Using the integration ratio of a signal distinctively attributed to the repeating unit versus one to the end groups,

(29) (a) Kajigaeshi, S.; Kakinami, T.; Yamasaki, H.; Fujisalio, S.; Okamoto, T. *Bull. Chem. Soc. Jpn.* **1988**, *61*, 600. (b) Kosynkin, D. V.; Tour, J. M. *Org. Lett.* **2001**, *3*, 991.

(30) (a) Matyjaszewski, K.; Xia, J. *Chem. Rev.* **2001**, *101*, 2921. (b) Kamigaito, M.; Sawamoto, M. *Chem. Rev.* **2001**, *101*, 3689. (c) Patten, T. E.; Matyjaszewski, K. *Adv. Mater.* **1998**, *10*, 901.

(31) (a) Coessens, V.; Matyjaszewski, K. *J. Macromol. Sci., Pure Appl. Chem.* **1999**, *A36*, 653. (b) Coessens, V.; Matyjaszewski, K. *J. Macromol. Sci., Pure Appl. Chem.* **1999**, *A36*, 811.

(32) (a) Matyjaszewski, K. *Macromolecules* **1998**, *31*, 4710. (b) Lutz, J.-F.; Matyjaszewski, K. *J. Polym. Sci., Part A: Polym. Chem.* **2005**, *43*, 89.

(33) (a) Coessens, V.; Pintauer, T.; Matyjaszewski, K. *Prog. Polym. Sci.* **2001**, *26*, 337. (b) Matyjaszewski, K.; Nakgawa, Y.; Gaynor, S. G. *Macromol. Rapid Commun.* **1997**, *18*, 1057. (c) Lutz, J.-F.; Borner, H. G.; Weichenhan, K. *Macromol. Rapid Commun.* **2005**, *26*, 514.

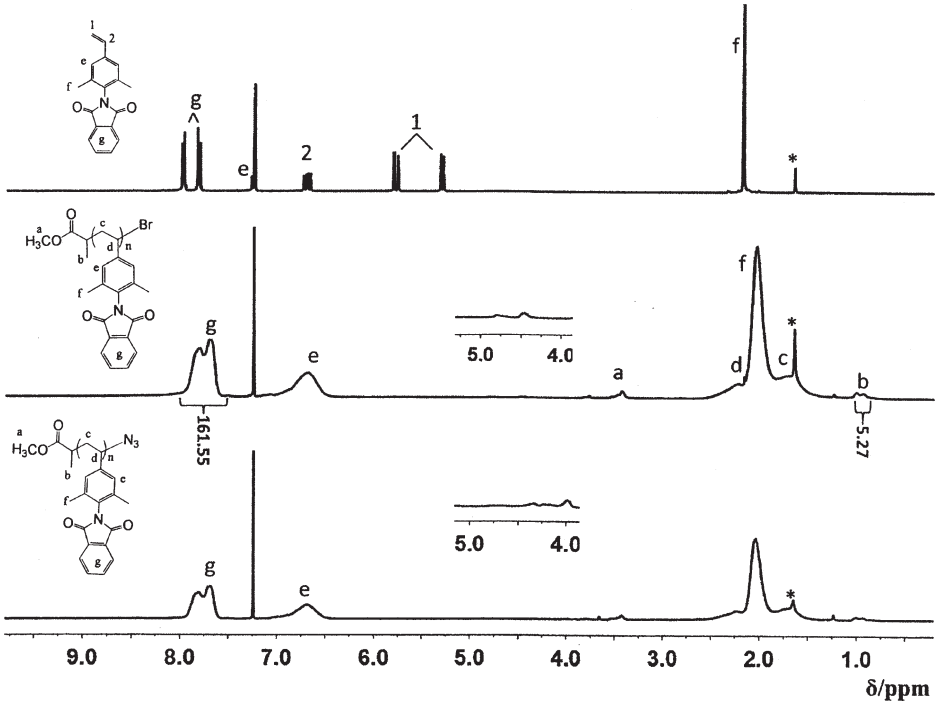

Figure 2. ^{1}H NMR spectra of monomer 2, PS-Br and PS-N_3 in $CDCl_3$.

Scheme 2. Synthesis of an Ethynyl-Terminated PPV Block

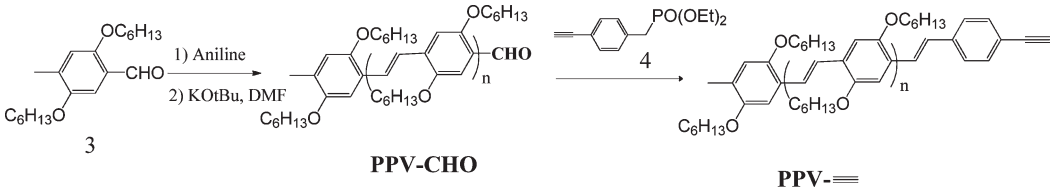

such as g versus b, one may calculate the degree of polymerization to be around 22.

The synthesis of an ethynyl-functionalized PPV block is shown in Scheme 2. A PPV block with one terminal aldehyde group was synthesized in one step via the Siegrist polycondensation of monomer **3**, an approach demonstrated previously by Kretzschmann et al. and Hadziioannou et al.[34] The PPV-CHO was converted to the ethynyl terminated PPV by Horner−Wittig−Emmons reaction with compound **4**.

Figure 3 shows the ^{1}H spectra of compound **3** and the two PPV polymers. After polymerization, two major peaks at 7.48 (8) and 7.15 (9) appeared, which are assigned to aromatic and vinyl protons, respectively. The methyl and aldehyde end groups (1 and 6) are clear. Other end group signals such as 2, 3, 4, 5, and so forth are also visible. Using the integration ratio of signal 7 versus 1 (7:1 = 76:1), one obtains the degree of polymerization around 11. After converting the aldehyde to alkyne, signals associated with the −CHO end such as 1, 2, 4, and so forth disappeared. Signals corresponding to the new end group, such as alkyne signal 1′ (3.12) are clear. Signals at the other end, such as 3, 5 are again clear with no change in chemical shift observed. Using the integration of signals 7 and 6 (7:6 = 60:2.5), a degree of polymerization of 11 is again obtained.

The azide terminated flexible coil block (PS-N_3) and ethynyl terminated rigid block (PPV−≡) were joined together through modified Huisgen 1,3-dipolar cycloaddition or simply "click" chemistry (Scheme 3). This reaction has gained a considerable amount of attention over the years because of its mild conditions, high yields, easy experimental set up, minimal synthetic workup, and tolerance of a wide variety of functional groups.[35] While PS-N_3 is soluble in common organic solvents such as chloroform, dichloromethane, dimethylformamide (DMF), dimethyl sulfoxide (DMSO), acetone, tetrahydrofuran

(34) (a) Stalmach, U.; de Boer, B.; Videlot, C.; van Hutten, P. F.; Hadziioannou, G. *J. Am. Chem. Soc.* **2000**, *122*, 5464. (b) Van der, V.; Marleen, H.; De Boer, B.; Stalmach, U.; Van de Wetering, K. I.; Hadziioannou, G. *Macromolecules* **2004**, *37*, 3673. (c) Kretzschmann, H.; Meier, J. *Tetrahedron Lett.* **1991**, *32*, 5059.

(35) (a) Kolb, H .C; Finn, M. G.; Sharpless, K. B. *Angew. Chem., Int. Ed.* **2001**, *40*, 2004. (b) Brase, G.; Gil, C.; Knepper, K.; Zimmermann, V. *Angew. Chem., Int. Ed.* **2005**, *44*, 5188. (c) Meldal, M.; Tomoe, C. W. *Chem. Rev.* **2008**, *108*, 2952. (d) Laurent, B. A.; Grayson, S. M. *J. Am. Chem. Soc.* **2006**, *128*, 4238. (e) Parrish, B.; Breitenkamp, R. B.; Emrick, T. *J. Am. Chem. Soc.* **2005**, *127*, 7404. (f) Joralemon, M.; O'Reilly, R. K.; Hawker, C. J.; Wooley, K. L. *J. Am. Chem. Soc.* **2005**, *127*, 16892. (g) Sumerlin, B. S.; Tsarevsky, N. V.; Louche, G.; Lee, R. Y.; Matyjaszewski, K. *Macromolecules* **2005**, *38*, 7540. (h) Golas, P. L.; Tsarevsky, N. V.; Matyjaszewski, K. *Macromol. Rapid Commun.* **2008**, *29*, 1167. (i) Droumaguet, B. L.; Velonia, K. *Macromol. Rapid Commun.* **2008**, *29*, 1073. (j) Binder, W. H.; Sachsenhofer, R. *Macromol. Rapid Commun.* **2007**, *28*, 15.

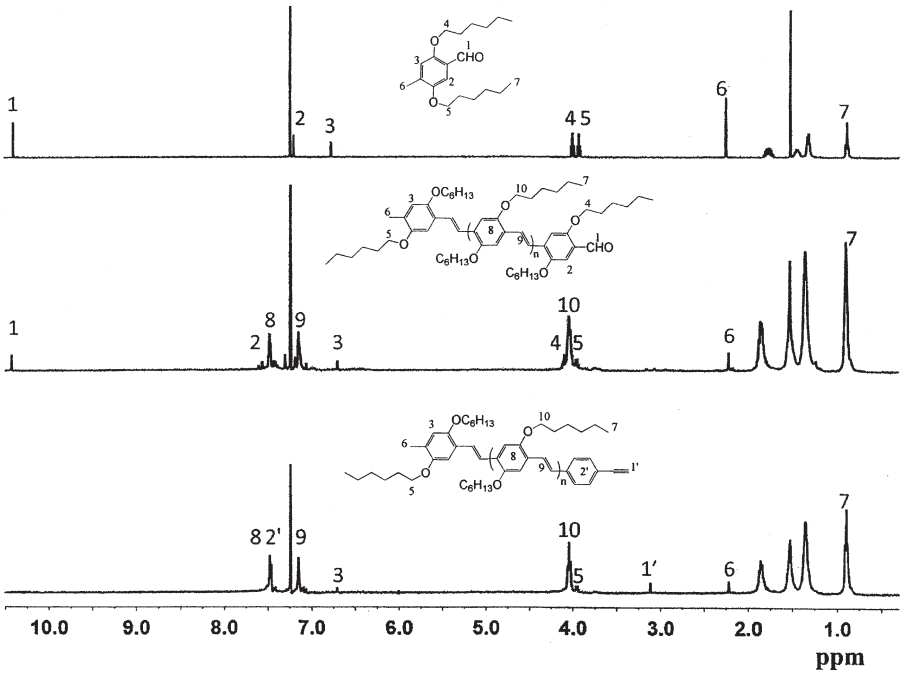

Figure 3. ^{1}H NMR spectra of monomer **3** and resulting PPV blocks in $CDCl_3$.

Scheme 3. Synthesis of the PS-PPV DCP and the Targeted Hybrid DCP

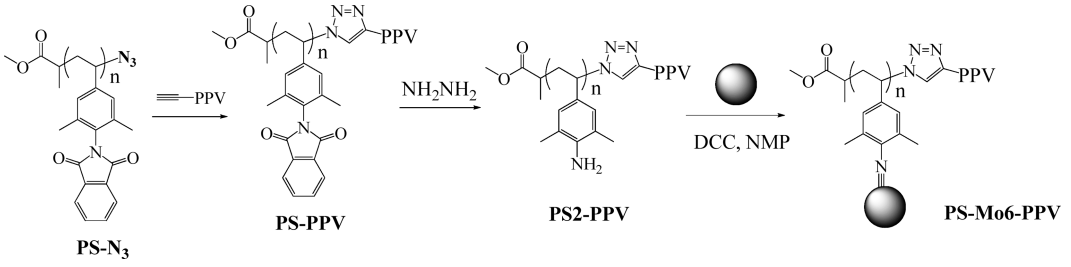

(THF), and so forth the PPV−≡ block is soluble only in chloroform, dichloromethane, and THF. The "click" reaction is thus carried out in THF. The resulting diblock copolymer PS-PPV is found to exhibit similar solubility to that of the PPV block, making the separation of any unreacted PPV block difficult. To ensure complete reaction of the PPV block, more than one equivalent of PS-N_3 block was used. The unreacted excess PS-N_3 block can be easily removed by precipitating the mixture from acetone: PS-N_3 is soluble in acetone while PS-PPV is not. As shown in Figure 4, the ^{1}H NMR spectrum of the "clicked-together" diblock copolymer is essentially a combination of the spectra of the two polymer blocks, except for the missing terminal alkyne proton signal (signals 1′). When the spectral region of 5−6 ppm is expanded, one can note a signal around 5.15 ppm which can be assigned to the proton associated with triazole-binding carbon in the PS block.[35h] Using the integration of signals attributed distinctively to either block, one can calculate the n/m ratio (n and m are the degree of polymerizations of the PS and PPV block, respectively). For example, using the integration of signals g (34) and 8 (8), the n/m ratio is calculated to be 2.1 to 1, consistent with the degrees of polymerization of the two blocks.

The protected amine group was made free with hydrazine hydrate according to the Ing−Manske procedure.[36] The complete removal of the protecting phthalimide groups is confirmed by the ^{1}H NMR spectrum of the resulting polymer (see Figure 4) where signal g is completely missing. The final cluster attachment was carried out in 1-methyl-2-pyrrolidinone (NMP) with excess hexamolybdate cluster and dicyclohexylcarbodiimide (DCC). Both the cluster and the PS-PPV DCP are soluble in NMP, and the cluster attachment reaction was followed by gel permeation chromatography (GPC). Excess free clusters after the reaction were removed by precipitating the polymer from hot acetonitrile. The resulting cluster-attached DCP is soluble in NMP, but only slightly soluble in chloroform and THF, and insoluble in most other organic solvents.

The ^{1}H NMR spectrum of the cluster-attached DCP was taken in $CDCl_3$. Because of its limited solubility, the spectrum reflects only the structures of those soluble DCPs. As shown in Figure 4, the spectrum shows rather weak aromatic signals. The broad signals e and f seen in the ^{1}H NMR spectrum of the deprotected DCP have disappeared. Weak but discernible signals seen at 6.92 and 2.80 ppm are likely downfield shifted signals e and f,

(36) (a) Khan, M. N. *J. Org. Chem.* **1996**, *61*, 8063. (b) Meuer, S.; Zentel, R. *Macromol. Chem. Phys.* **2008**, *209*, 158.

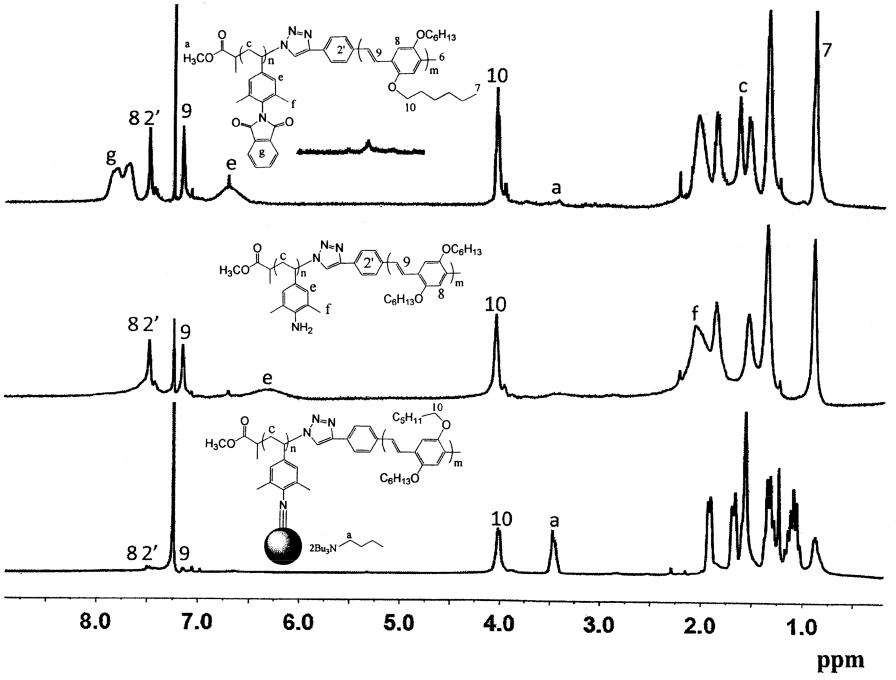

Figure 4. ^{1}H NMR of the PS-PPV DCP, the deprotected DCP, and the cluster attached DCP in $CDCl_3$.

respectively. The hybrid DCPs which are soluble in chloroform are likely to have only short PS segments which may account for the unusually low intensity of proton signals associated with the PS segment. New signals corresponding to the tetrabutylammonium counterion, such as the one at 3.42 ppm, appeared in the ^{1}H NMR spectrum of the cluster-attached DCP. While signals overlap extensively in the 1.0 to 2.0 region and the aromatic region, in the 3.0 to 5.0 ppm range, one observes two strong well-resolved broad signals at 4.05 and 3.42 ppm, which can be assigned to the $-OCH_2-$ proton of the PPV block and the $-NCH_2-$ protons of the tetrabutylammonium counterion, respectively. On the basis of their 1:1 integration ratio, one can estimate that the number of attached clusters is about one-fourth of the degree of polymerization (the *m* value shown in Figure 4) of the PPV block, which yields about 3 POM clusters per PS block.

Molecular Weights. Figure 5 shows the gel-permeation chromatography traces of the rigid PPV block, the PS block, the PS-PPV DCP, free cluster [Mo6], and the hydrid DCP. All measurements were run at 30 °C using THF as the eluent. The coil PS block has a number average molecular weight (M_n) of 2732 and a polydispersity (PD) of 1.10. The relatively narrow molecular weight distribution indicates the living nature of the polymerization. The PPV block has a M_n of 2208 and a slightly larger PD of 1.27. Such a PD is consistent with literature reports.[34b] After "click" coupling, the PS-PPV DCP shows a M_n of 5900 and a PD of 1.22. No uncoupled PPV block or PS block is seen in the DCP's GPC trace, indicating a complete coupling reaction. Such a result also confirms that all the PS coil blocks prepared from the ATRP process possess the active Br end group. After cluster attachment, the resulting hybrid DCP shows a peak with a significantly

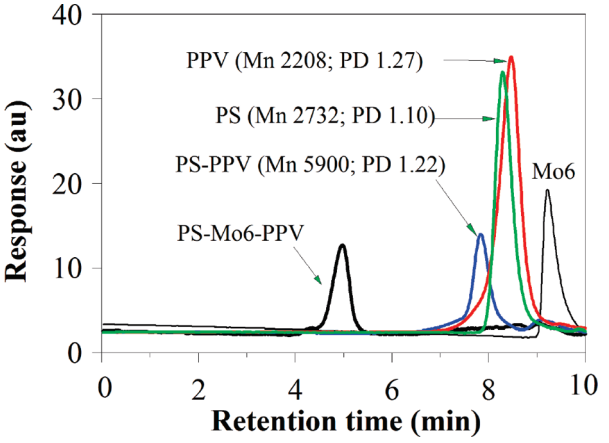

Figure 5. GPC traces of the PS-Br block, the PPV−≡ block, the PS-PPV DCP, and the hybrid DCP using THF as the eluent.

shortened retention time. No peaks corresponding to the unreacted DCP and the free [Mo6] cluster are observed, indicating that all DCPs have reacted and free clusters have completely washed out. While one cannot conclude that all amines have reacted and most likely that will not happen because of steric reasons, the narrow PD of the resulting hybrid DCP indicates that the extent of functionalization is fairly consistent among different DCP chains.

Realizing that GPC produces only a relative molecular weight (in relation to polystyrene standards), matrix-assisted laser desorption/ionization-Time-of-Flight (MALDI-TOF) mass spectrometry (MS) measurements were also carried out on all polymers to yield information on their absolute molecular weights and molecular weight distributions. As shown in Figure 6, MALDI-TOF spectra of PS-**Br** and **PS-N$_3$** show a regularly distributed set of peaks with mass difference of one repeating unit (277.11). On the basis of the molecule weights and the

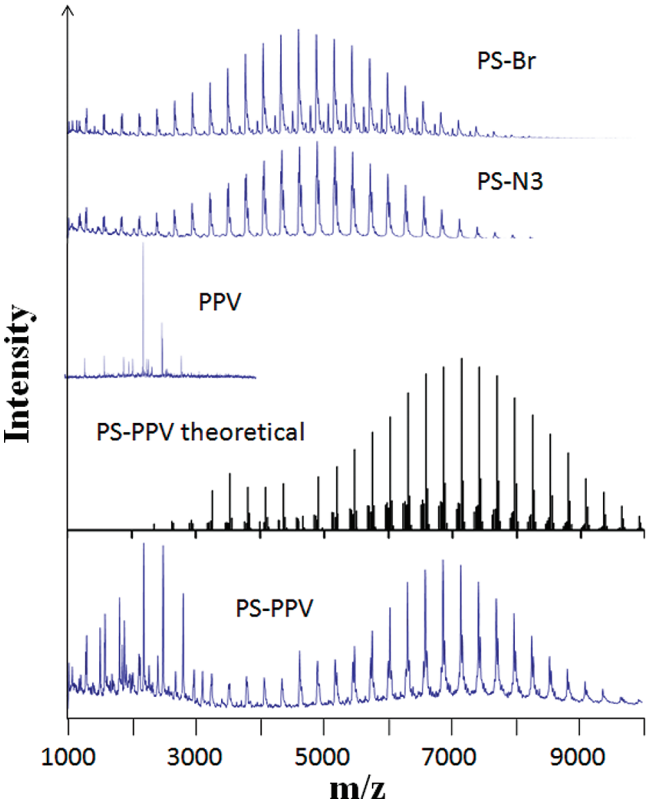

Figure 6. MALDI-TOF spectra of the PS block, the PPV block, and the PS-PPV DCP. The theoretical MW distribution is calculated based on the random statistical reaction of the two blocks with the shown MW distribution.

intensities of peaks, one can calculate the M_n of **PS-Br** and **PS-N_3** to be 4494 and 4596, respectively, which corresponds to an average degree of polymerization (DP) of 18, reasonably consistent with the DP obtained by ^{1}H NMR. Both polymers show narrow molecular weight distributions with PD of 1.10 and 1.11, respectively, confirming the living nature of the polymerization. The MALDI-TOF spectrum of the PPV block shows one major peak at a mass/charge ratio of 2209.8, corresponding to 7 repeating units. The M_n and PD of PPV are calculated to be 2116 and 1.03, respectively. After being clicked together, the resulting DCP shows a M_n of 6644 and a PD of 1.04. The molecular weight of PS-PPV DCP matches very well with the theoretical value of 6712 (4596 + 2116) calculated based on the M_n's of the two blocks. Taking the distributions of the PS-N_3 block and the PPV block and assuming a random reaction between them, the theoretical statistical molecular weight distribution of the PS-PPV DCP is calculated and shown in Figure 6 as well. One sees a nice match between the theoretical prediction and the actual experimental results, confirming the diblock copolymer formation. It is noted that a lower molecular weight distribution in the 1000−3000 range is observed, which was initially attributed to any unreacted PPV block. Repeated attempts in chromatography separation failed to remove these low molecular weight components. Since GPC trace of PS-PPV does not show a corresponding low molecular distribution, it is possible that those low molecular weight components are fragments of PS-PPV, generated during the MS measurements.

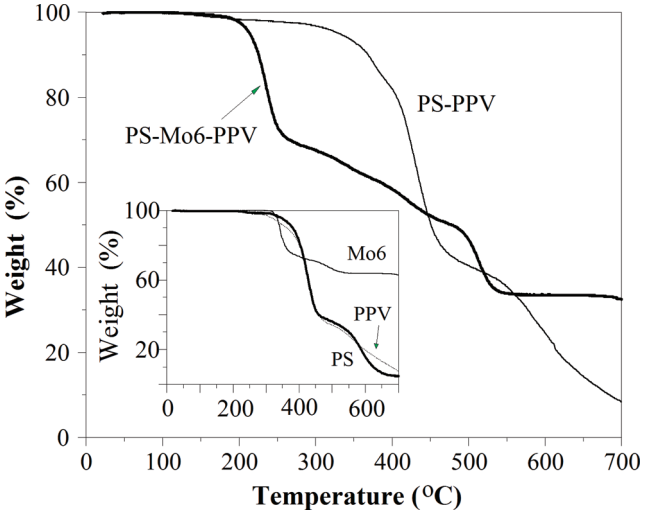

Figure 7. TGA thermograms of PS-Br, PPV−≡, PS-PPV DCP, $[Mo_6O_{19}]\cdot 2NBu_4$ cluster, and the hybrid DCP.

While MALDI-TOF measurements yield molecular weight information for the PS block, PPV block and the PS-PPV DCP. The MALDI-TOF spectra of the cluster-attached DCP revealed no peaks beyond a mass/charge ratio of 3000, whether using a positive or negative detection mode. The lack of high mass/charge signals may be due to the difficulty in vaporizing cluster-attached DCPs under the MALDI conditions or due to the simple fact that the hybrid DCP is highly charged (as each attached cluster carried a −2 charge).

Thermal Properties. Thermal properties of the two blocks, PS-PPV DCP and the hybrid DCP were studied by thermogravimetric analysis (TGA), and the results are shown in Figure 7. While both the cluster and the PS-PPV DCP are thermally stable up to 300 °C, the hybrid DCP started to decompose at a much lower temperature of 200 °C. Weight loss continued until 530 °C when no further loss is observed up to 700 °C. A residual weight of 34% remains. For the free Mo6 cluster, a similar no weight loss region from 530 to 700 °C is observed, and the residual weight is 64%, which is consistent with its cluster anion content of 64%. The PS block, the PPV block, and PS-PPV, on the other hand, all started to degrade around 300 °C and continued to lose weight up to 700 °C. All these polymers have less than 8% residual weight at 700 °C. It is thus reasonable to assume that at 700 °C, the thermally decomposed residue of the hybrid DCP is MoO_3, from which one can calculate the weight percentage of Mo in the hybrid DCP to be 22%. Using the DPs of 18 and 7, obtained from the above MALDI-TOF measurements, for the PS and PPV blocks, respectively, and assuming a complete phthalimide deprotection, a 22% Mo content in the hybrid DCP indicates that the number of attached clusters per PS block is between 3 (20% Mo) and 4 (23% Mo), quite consistent with the result obtained from ^{1} H NMR studies.

IR Spectra. Both ^{1}H NMR and TGA analysis confirm the existence of clusters in the hybrid DCP, and GPC indicates that those clusters are attached covalently to the DCP polymer. The cluster attachment is also confirmed

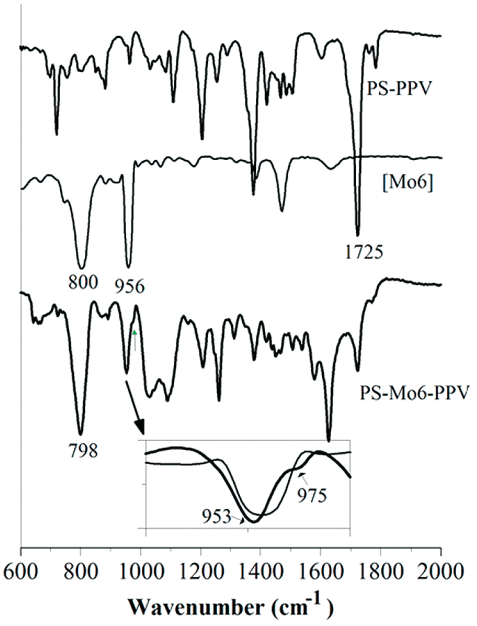

Figure 8. IR spectra of the PS-PPV DCP, free Mo6 cluster, and the hybrid DCP.

by IR measurements. As shown in Figure 8, the PS-PPV DCP shows a sharp and intense peak at 1725 cm^{-1} which can be assigned to the carbonyl stretching of the phthalimide protecting group. After deprotection and cluster attachment, this peak is significantly weakened. On the other hand, new peaks at 798 and 953 cm^{-1}, which are characteristic Mo−O stretching vibrations, are shown clearly in the IR spectra of the hybrid DCP. One also notes a side/shoulder peak next to 953 cm^{-1}, which can be seen more clearly when expanded. This peak is attributed to the Mo−N stretching vibration.[28b] The observation of this peak is a good indication that Mo6 clusters are attached to the coil block.

Electrochemistry. Cyclic voltammetry measurements of the DCP and hybrid DCP were carried out in acetontrile using a Pt-disk working electrode coated with the respective polymer film. Under identical conditions, a reversible oxidation wave at 0.32 eV is observed for the ferrocene/ferrocenium couple. As shown in Figure 9, the cyclovoltammogram of the hybrid DCP shows clearly a reduction process around −1.1 eV which does not exist in the precursor DCP, and is cathodically shifted compared to that of free [Mo6]. This reduction process can be attributed to the imido-POM clusters, which are known to exhibit higher reduction potentials (more difficult to be reduced) than the free Mo6 cluster.[7,37] The clear observation of this reduction wave and the absence of reduction process of free clusters indicate that all POM clusters in the hybrid DCP are covalently bonded to the coil block through the imido Mo−N bond. Both the PS-PPV DCP and the hybrid DCP show a semi-reversible reduction process at around −1.5 eV, which is due to the reduction of the PPV block.

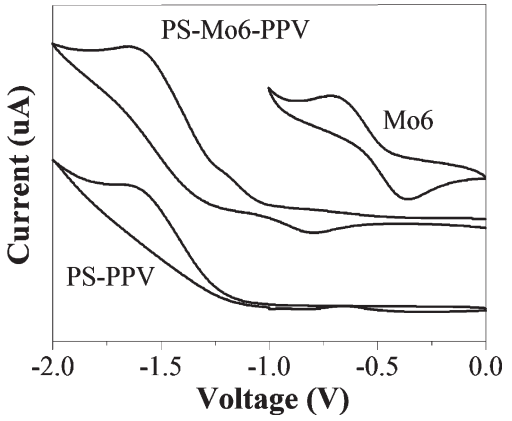

Figure 9. Cyclic voltammograms of the PS-PPV DCP, free Mo6 cluster, and the hybrid DCP.

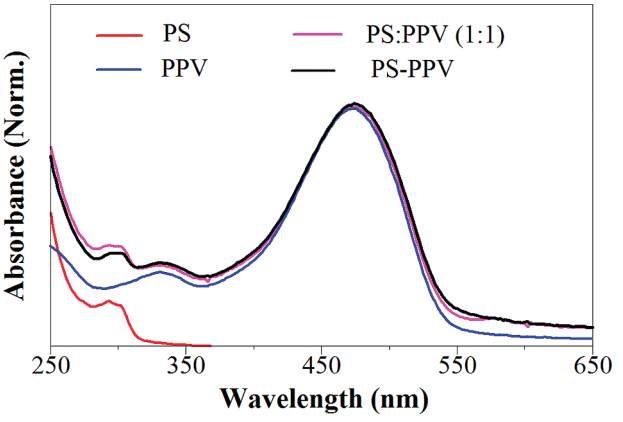

Figure 10. UV/vis absorption spectra of PS-Br, PPV−≡, a 1:1 PS/PPV mixture, and the PS-PPV DCP in dilute chloroform solutions.

Optical Properties. Figure 10 shows the absorption spectra of the PS block, PPV block, a 1:1 PS/PPV mixture and the "click" coupled DCP. The absorption spectrum of the DCP closely matches that of the 1:1 PS/PPV mixture in both the UV and the visible region, indicating again a complete coupling between the two blocks. It also implies that there are minimal electronic interactions between the two blocks in their ground states. After cluster attachment, a new peak at around 370 nm appeared while the λ_{max} in the visible region is blue-shifted (Figure 11). The new peak at 370 nm matches well with the absorption spectrum of the imido-POM derivative of 2,6-dimethylaniline,[38] and can thus be assigned to the ligand-to-metal charge-transfer (LMCT) transition of the pendant imido-POM component. The observation of this peak indicates clearly the formation of imido-functionalized POM clusters, again confirming the covalent cluster attachment. The absorption band in the visible region of the hybrid DCP is due to the $\pi-\pi^*$ transition of the PPV block. The slight blue shift of this band, compared to that of PS-PPV DCP, indicates that the attachment of POM clusters to the coil block has some effect on the effective conjugation length of the PPV block. It is possible that the

(37) Strong, J. B.; Yap, G. P. A.; Ostrander, R.; Liable-Sands, L. M.; Rheingold, A. L.; Thouvenot, R.; Gouzerh, P.; Maatta, E. A. *J. Am. Chem. Soc.* **2000**, *122*, 639.

(38) Li, Q.; Wu, P.; Wei, Y.; Wang, Y.; Wang, P.; Guo, H. *Inorg. Chem. Commun.* **2004**, *7*, 524.

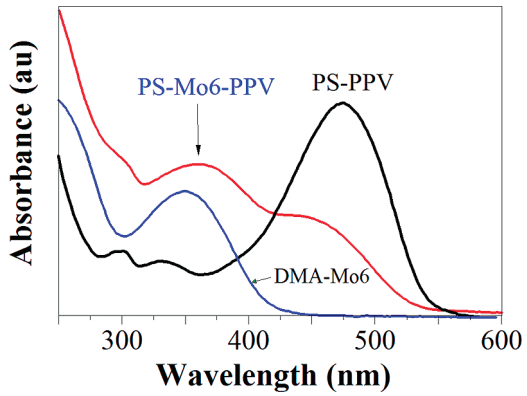

Figure 11. UV/vis spectra of the PS-PPV DCP, the hybrid DCP, and the 2,6-dimethylaniline functionalized hexamolybdate cluster in dilute chloroform solutions.

bulky cluster-containing PS block may twist the bridging phenylene vinylene segment and thus decreases the effective conjugation length of the PPV block.

Both the DCP and hybrid DCP exhibit strong fluorescence in dilute solutions. Their fluorescence quantum yields are 0.21 and 0.19, respectively, indicating negligible fluorescence quenching in solution after cluster attachment. This observation is consistent with our previous report on side chain POM-containing conjugated polymers where POM clusters exhibit inefficient fluorescence quenching when they are linked to the conjugated backbone through flexible alkyl bridges.[28b] In the hybrid DCP, the POMs are further away from the PPV donor and thus photoinduced electron-transfer from PPV to POM is kinetically hampered. In the solid film, however, hybrid DCP does show much weaker fluorescence. Compared to PPV and PS-PPV, whose films show FL quantum yields of 0.48 and 0.34, respectively, hybrid DCP shows a fluorescence quantum yield of only 0.09, indicating the quenching of 74% of the PPV fluorescence when compared to PS-PPV. It is noted that while PS-PPV shows identical fluorescence to that of PPV in dilute solution, the emission of PS-PPV films is red-shifted by 15 nm while the hybrid DCP blue-shifted by 10 nm, as shown in Figure 12. Clearly, the PPV segments aggregate quite differently after the cluster attachment. Since the PPV emission in the hybrid DCP is not as red-shifted as that in PS-PPV, the observed fluorescence quenching of hybrid DCP may not be attributed to a better PPV π-stacking. The more plausible cause is the photoinduced electron transfer from the PPV exciton to the POM clusters. Such an electron transfer becomes facile in the solid state because of the close proximity of the donor PPV of one DCP and the acceptor POM clusters of another DCP. In other words, the inefficient intrapolymer photoinduced electron transfer in a dilute solution is replaced with efficient interpolymer electron transfer in the solid state, which accounts for the observation that the hybrid DCP is highly fluorescent in dilute solutions but exhibits much weaker fluorescence in the solid state.

Film Morphologies. Chloroform solutions of PPV, PS-PPV, and the hybrid DCP (1 mg in 1 mL chloroform) were spin-coated onto silicon wafer at a spin rate of 3000

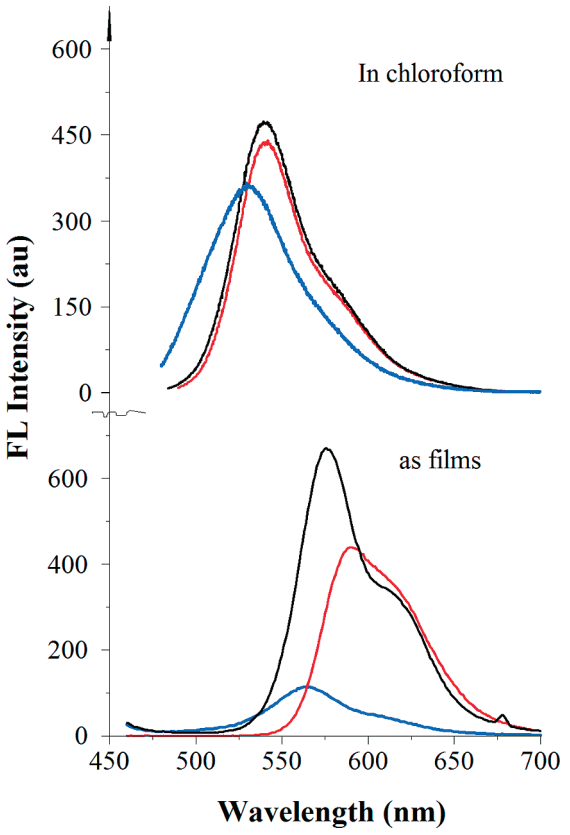

Figure 12. Fluorescence emission spectra of PPV (black), PS-PPV (red), and the hybrid DCP (PS-Mo6-PPV, blue) in dilute chloroform solutions and as solid films.

and 1500 rpm. After drying in a vacuum oven overnight, the films were sputter-coated with a thin layer of gold/palladium. Field-emission scanning electron microscope (SEM) XL30 (FEI Company, Hillsboro, OR) was used with an accelerating voltage of 15.0 kV. The SEM images (Figure 13) of the PS-PPV films show interesting microporous structures. At a high spin rate, the pores have irregular shape and varied sizes. At a spin rate of 1500 rpm, the pores show a regular spherical shape and much more uniform size. The average diameter of the pores is around 500 nm. While a number of rod−coil diblock copolymers have been shown to give microporous films,[42] such morphologies are usually obtained by drop-casting with slow evaporation of the solvent. The formation of microporous films by spin-coating indicates that the PS-PPV DCP self-assembles rather quickly as solvent evaporates. Insights into the self-assembly process and the micropore formation mechanism require a detailed and systematic study of how the block sizes, solvent, polymer concentration, spin rate, thermal treatment, and so forth affect the film morphologies. Such studies are currently in progress. After cluster attachment, the resulting hybrid DCP yields films with very different morphologies. As shown in Figure 13 (c and d), spin-coating of a hybrid DCP solution gives films with an uneven surface and non-uniform coverage. While one sees pits in the film and some areas of aggregated lumps, the widespread pores seen in the DCP film are clearly missing. When the smooth film area is magnified, one sees no phase separated domains. It should be noted

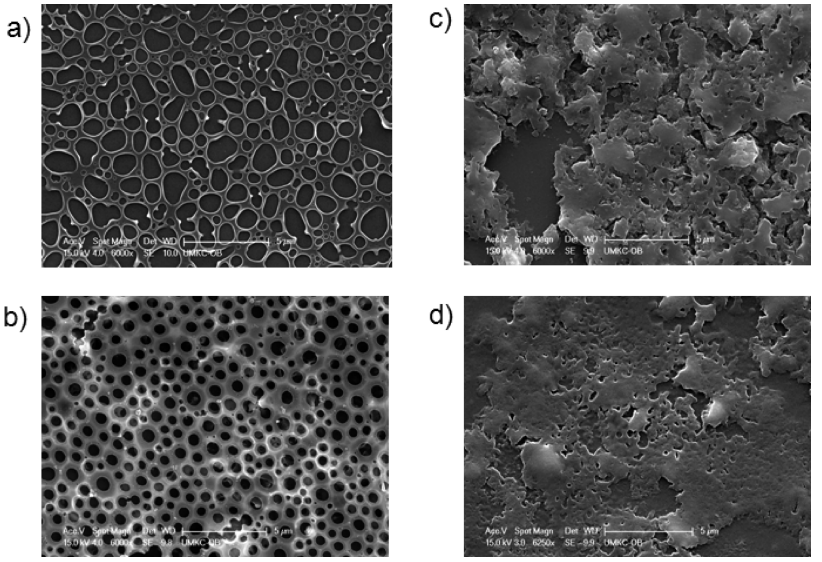

Figure 13. SEM images of PS-PPV films (a,b) and the hybrid DCP fims (c, d), spin-coated at spin rates of 3000 rpm (a and c) and 1500 rpm (b and d).

that the morphology of a spin-coated pristine film is formed through a kinetic process rather than a thermodynamic one, and thus it may be altered with time and temperature. The actual morphology depends on several factors like choice of solvent, annealing temperature, drying speed, and, above all, the degree of polymerization of each block. In our preliminary morphology studies, chloroform, a good solvent for both blocks, was used as the solvent. It remains to be seen whether a good solvent for only one of the blocks will be able to create any new type of morphology. While no phase-separated morphologies were observed for either the PS-PPV DCP or the hybrid DCP films without prior thermal treatment, we are currently exploring the film morphologies spin-coated from different solvents, under different spin rates and after thermal annealing at various temperatures.

Conclusions

In conclusion, we have successfully prepared the first POM-containing DCP through the post-polymerization functionalization approach. Click chemistry was used to join together a rigid PPV block and a flexible PS block to form the precursor DCP. Both GPC and MALDI-TOF measurements have confirmed the formation of the DCP with a narrow molecular weight distribution. POM cluster attachment was carried out in NMP, a solvent in which both the precursor DCP and the Mo6 cluster are soluble. The cluster attachment was confirmed by GPC, IR, CV, and optical spectroscopy. The hybrid DCP shows two absorption bands, one at 450 nm due to $\pi-\pi^*$ transition of the PPV block, and the other at 370 nm attributable to the ligand-to-metal charge transfer transition of functionalized Mo6 clusters. Spin-coated PS-PPV films show microporous structures which are not observed in the hybrid DCP films. Significant fluorescence quenching is observed for the hybrid DCP because of photoinduced electron transfer from the PPV exciton to POM cluster, indicating its potential as photovoltaic materials. To realize the desired morphology for photovoltaic applications, we are currently synthesizing POM-containing DCPs with different block structures, longer block lengths, and different volume fractions of each block.

Experimental Section

Materials. Triethylamine was distilled over CaH_2. THF was purified by distillation over sodium pellets and benzophenone. CuBr was purified by washing consecutively with glacial acetic acid, absolute ethanol and ethyl ether, and then dried under vacuum. *N*,*N*,*N*′,*N*′,*N*″-pentamethyldiethylenetriamine (PMDETA, 99%), methyl-2-bromopropionate, aniline, 1-methyl-2-pyrrolidinone, and *p*-xylene were distilled in vacuo before use. All other chemicals were purchased either from Aldrich or Acros and were used as received unless otherwise stated. Compound **1**[28b] and **3**[39] were prepared according to literature procedures. Compound **4** was prepared in three steps by benzylic bromination of 4-iodotoluene[40] followed by Arbuzov reaction and Sonogashira coupling reaction with trimethylsilylacetylene.[41]

Instrumentation. All reactions were conducted under the protection of nitrogen. The ^{1}H and ^{13}C NMR spectra were collected on a Varian INOVA 400 MHz FT NMR spectrometer. All samples were referenced to the deuterated solvents. GPC measurements were performed at 30 °C on a Waters system equipped with a Waters 410 differential refractometer, Waters 515 HPLC pump, and a styragel HR 4E column with THF as the eluent. The calibration curve was determined by the use of five polystyrene standards from 800 to 90,000. FT-IR spectra were obtained from samples dispersed on KBr pellets on an IR100 FT-IR spectrometer (Thermo-Nicolet Co.). UV−vis absorption spectra were measured on a Hewlett-Packard 8452A diode array spectrophotometer, and photoluminescence spectra were measured using a Shimadzu RF-5301PC spectrofluorophotometer. Fluorescence quantum yields for solution were determined

(39) Gu, T.; Nierengarten, J.-F. *Tetrahedron Lett*. **2001**, *42*, 3175.
(40) Wilson, A. A.; Dannals, R. F.; Ravert, H. T.; Frost, J. J.; Wagner, H. N. *J. Med. Chem*. **1989**, *32*, 1057.
(41) Xiao, J.; Li, J.; Li, C.; Huang, C.; Li, Y.; Cui, S.; Wang, S.; Liu, H. *Tetrahedron Lett*. **2008**, *49*, 2656.
(42) (a) Lee, M.; Cho, B. -K.; Zin, W.-C. *Chem. Rev*. **2001**, *201*, 3869. (b) Jenekhe, S. A.; Chen, X. L. *Science* **1999**, *283*, 372. (c) Lin, C. L.; Tung, P. H.; Chang, F. C. *Polymer* **2005**, *46*, 9304.

using quinine sulfate in 1 N H_2SO_4 ($\varphi_{fl} \approx 0.55$) as the standard. For films, diphenylanthracene (dispersed in PMMA film with concentration less than 10^{-3} M, assuming PL efficiency of 0.83) was used as the standard. Cyclic Voltammetry (CV) studies were carried out in acetonitrile at room temperature under argon protection using a BAS Epsilon EC electrochemical station employing a 1 mm^2 Pt disk as the working electrode, silver wire as the reference electrode, and a Pt wire as the counter electrode. $[Bu_4N]PF_6$ was the supporting electrolyte, and the scan rate was 50 mV/s. Polymer films were cast from chloroform onto the Pt disk working electrode. Ferrocene was used as an internal standard. Thermal analyses were performed on Shimadzu TGA-60 at the heating rate of 10 °C/min. A Voyager DE Pro (Perceptive Biosystems/ABI) MALDI-TOF mass spectrometer was used for mass measurement, operating in both linear and reflector mode. A mixture of silver trifluoroacetate/dithranol (1, 8-dihydroxyanthrone) (1:25 w/w) was used as the matrix.

Sample Preparation for SEM. One mg of each of the three polymer samples was dissolved separately in 1 mL of chloroform solution inside a glovebox. Though PPV and PS-PPV were readily soluble in chloroform, hybrid DCP were heated at 50 °C and stirred overnight under nitrogen protection to make a homogeneous solution. The solutions were filtered through 0.45 μm PTFE filter prior to spin coating on silicon wafers at spin rates of 3000 or 1500 rpm. All the films were dried in a vacuum oven overnight and then sputter-coated with a thin layer of gold.

Compound 2. Compound **1** (8.95 g, 23.7 mmol) and tetrakis (triphenylphosphine) palladium (0) (0.522 g, 0.435 mmol) were added into a 100 mL two-neck flask. The flask was evacuated and backfilled with nitrogen three times. Tributyl (vinyl) tin, (97%, 7.75 g, 24.4 mmol) and DMF were then added dropwise to the flask with a syringe. The resulting mixture was stirred at 100 °C for 3 h and then poured into water. The solution was extracted with methylene chloride (3 × 300 mL). The organic layer was collected, washed with water (3 × 300 mL), and dried over magnesium sulfate. The solvent was evaporated to yield a yellow crude product, which was purified by column chromatography (silica gel, hexane/methylene chloride 4:1 as the eluent) to afford compound **2** as a white solid (4.00 g, 60%, mp 186−188 °C). ^{1}H NMR (400 MHz, $CDCl_3$, 25 °C): δ 7.95 (m, 2H), 7.79 (m, 2H), 7.21 (s, 2H), 6.67 (dd, J = 10.8 Hz, 17.6 Hz, 1 H), 5.75 (dd, J = 0.8 Hz, 17.6 Hz, 1H), 5.27 (dd, J = 0.8 Hz, 10.8 Hz, 1H), 2.14 (s, 6 H). ^{13}C NMR ($CDCl_3$, 400 MHz): δ 167.2, 138.6, 136.9, 136.1, 134.3, 131.9, 129.1, 126.3, 123.8, 115.0, 18.1. Anal. Calcd. For $C_{18}H_{15}NO_2$: C, 77.90; H, 5.45; N, 5.05. Found: C, 77.65; H, 5.33; N, 5.17.

PPV-CHO. Synthesis of Poly(2,5-Dihexyloxy-1,4-phenylene-vinylene). Compound **3** (1.46 g, 4.68 mmol) was added into a two-neck flask. The flask was evacuated and backfilled with nitrogen three times. To the flask was added a sample of aniline (0.480 g, 5.15 mmol) with a nitrogen-filled syringe. The reaction mixture was stirred at 60 °C for 1.5 h. Potassium *tert*-butoxide (1.05 g, 9.36 mmol) was then added into the above mixture, followed by dry DMF (36 mL). The resulting reaction mixture was stirred at 80 °C under nitrogen for 3 h. After being cooled down to room temperature, the solution was poured into a mixture of 150 mL of 1 N HCl and 200 mL of $CHCl_3$ to hydrolyze the aldimine end group. After the mixture was stirred for 1 h, the organic layer was collected and washed with water until the aqueous phase was neutral. The organic layer was dried over sodium sulfate. After stripping off most of the solvent, the concentrated residue solution was poured into a large excess of acetone. The resulting dark red precipitates were filtered and dried at 50 °C under vacuum to give 1.2 g of product (yield 55%). ^{1}H NMR (400 MHz, $CDCl_3$, 25 °C): δ 10.43 (s, 1H), 7.48 (m, 16H), 7.15 (m, 14H), 6.71 (s, 2H), 4.04 (br), 2.22 (s, 3H), 1.84 (br), 1.53 (br), 1.35 (br), 0.89 (br). ^{13}C NMR ($CDCl_3$, 400 MHz): δ 189.2, 156.3, 151.1, 127.1, 123.0, 110.4, 69.5, 31.7, 29.5, 26.0, 22.7, 14.1. Anal. Calcd. For $C_{162}H_{244}O_{17}$: C, 78.91; H, 9.98. Found: C, 77.63; H, 9.92. GPC: M_n = 2208, PDI = 1.27. MALDI MS: M_n = 2116, PDI = 1.03.

PPV−≡. PPV-CHO (0.600 g) was added into a two-neck flask, and the flask was evacuated and then backfilled with nitrogen three times. Dry THF (20 mL) was then added, followed by sodium hydride (0.08 g, 3.33 mmol). After stirring at room temperature for 5 min, compound **4** (0.075 g, 0.297 mmol) in dry THF (5 mL) was then added dropwise to the above solution, and the resulting reaction mixture was refluxed for 16 h. The solution was then poured into water (50 mL) and extracted with chloroform. The organic layer was washed with water (100 mL) and dried over magnesium sulfate. After stripping the majority of the solvent, the concentrated solution was poured into methanol to yield the polymer as red solids, which were dried at 50 °C under vacuum (0.700 g, 90%). ^{1}H NMR (400 MHz, $CDCl_3$, 25 °C): δ 7.48 (m, 19H), 7.15 (m, 12H), 6.71 (s, 2H), 4.04 (br), 3.12 (s, 1H), 2.22 (s, 3H), 1.86 (br), 1.53 (br), 1.36 (br), 0.90 (br). ^{13}C NMR ($CDCl_3$, 400 MHz): δ 151.1, 132.4, 127.6, 126.3, 124.8, 123.2, 110.4, 69.5, 31.7, 29.5, 26.0, 22.7, 14.1. Anal. Calcd. For $C_{169}H_{248}O_{16}$: C, 79.97; H, 9.85. Found: C, 76.40; H, 9.51. GPC: M_n = 2208, PDI = 1.27. MALDI MS: M_n = 2110, PDI = 1.03.

PS-Br Block (ATRP of Compound 2). Compound **2** (0.500 g, 1.803 mmol) and CuBr (0.006 g, 0.041 mmol) were added to flame-dried two-neck round-bottom flask. The flask was degassed and backfilled with nitrogen three times, and left under nitrogen. Then PMDETA (0.009 mL, 0.008 g, 0.041 mmol) was added via a gastight syringe, followed by *p*-xylene (0.900 mL). After addition, three freeze−pump−thaw cycles were performed, and the mixture was allowed to stir at room temperature for 45 min under nitrogen. The solution became light green. The flask was then placed into an oil bath at 110 °C, and deoxygenated methyl-2-bromopropionate (0.005 mL, 0.007 g, 0.041 mmol) was added through a gastight micro liter syringe to initiate the polymerization. After 11 h, the contents of the flask were exposed to air to quench the polymerization. THF (30 mL) was then added to the flask to dissolve the polymer. The solution was then filtered through neutral alumina to remove the copper catalyst. The resulting colorless polymer solution was concentrated and twice precipitated into 10-fold excess of methanol. The white polymer was collected by vacuum filtration and dried under vacuum for 12 h (0.600 g). ^{1}H NMR (400 MHz, $CDCl_3$, 25 °C): δ 7.80 (br), 7.71 (br), 6.69 (br), 3.42 (br), 2.03 (br), 1.7 (br), 1.00 (br). ^{13}C NMR ($CDCl_3$, 400 MHz): δ 167.0, 145.9, 136.2, 133.9, 132.2, 127.8, 123.4, 40.4, 18.0. Anal. Calcd. For $C_{328}H_{277}N_{18}O_{38}Br$: C, 76.36; H, 5.41; N, 4.88. Found: C, 74.44; H, 4.67; N, 4.75. GPC: M_n = 2732, PD = 1.10. MALDI-TOF MS: M_n = 4494, PD = 1.10.

PS-N_3. PS-Br block (0.500 g, 0.164 mmol), sodium azide (0.032 g, 0.492 mmol), and DMF (4.00 mL) were added in a two-neck flask. The resulting solution was stirred at room temperature for 14 h. The reaction mixture was then precipitated into cold methanol (50 mL). The white solid was collected by vacuum filtration and washed with water. The solid was dried under vacuum. (0.450 g). ^{1}H NMR (400 MHz, $CDCl_3$, 25 °C): δ 7.80 (br), 7.71 (br), 6.65 (br), 3.37 (br), 2.03 (br), 1.70 (br), 0.93 (br). ^{13}C NMR ($CDCl_3$, 400 MHz): δ 167.0, 146.5, 136.3, 133.9, 132.2, 127.7, 123.5, 40.6, 18.1. Anal. Calcd. For $C_{328}H_{277}N_{21}O_{38}$: C, 76.90; H, 5.45; N, 5.75.

Found: C, 75.40; H, 4.89; N, 5.21. GPC: M_n = 2700, PDI = 1.10. MALDI MS: M_n = 4537, PDI = 1.11.

PS-PPV. PS-N_3 (0.092 g, 0.031 mmol) and CuBr (0.005 g, 0.035 mmol) were charged to a two-neck flask. The flask was then evacuated and backfilled with nitrogen three times. PMDETA (0.007 mL, 0.006 g, 0.035 mmol) and freshly distilled THF (15 mL) were then added to the above mixture. To the resulting light yellow homogeneous solution was added dropwise a THF solution of PPV−≡ (0.060 g, 0.024 mmol in 15 mL of THF). The resulting red solution was stirred at 45 °C for 24 h. The reaction mixture was filtered through neutral alumina to remove the copper catalyst. The resulting red solution was concentrated and precipitated into methanol (100 mL). The crude red solid was collected by vacuum filtration and washed with acetone to remove excess PS-N_3. The red solid was dried under vacuum at 50 °C (0.182 g, 90%). ^{1}H NMR (400 MHz, $CDCl_3$, 25 °C): δ 7.78 (br), 7.65 (br), 7.43 (br), 7.11 (br), 6.66 (br), 3.99 (br), 2.17 (br), 1.99 (br), 1.81 (br), 1.60 (br), 1.54 (br), 1.30 (br), 0.85 (br). ^{13}C NMR ($CDCl_3$, 400 MHz): δ 167.0, 151.0, 136.3, 133.9, 132.2, 127.6, 123.5, 110.4, 69.4, 40.6, 31.7, 29.5, 26.0, 22.7, 18.1, 14.1. Anal. Calcd. For $C_{497}H_{525}N_{21}O_{54}$: C, 77.80; H, 6.91; N, 3.44. Found: C, 77.44; H, 6.96; N, 2.80. GPC: M_n = 5900, PDI = 1.22. MALDI MS: M_n = 6644, PDI = 1.04.

Deprotection of Phthalimide Group. PS-PPV DCP (0.050 g, 0.008 mmol) was dissolved in freshly distilled THF in a two-neck flask. Then hydrazine monohydrate (0.200 g, 3.99 mmol) was added dropwise into the above red solution with constant stirring, and the entire reaction mixture was refluxed for 13 h under nitrogen protection. The resulting solution was cooled to room temperature, and the light orange-white precipitate was filtered off. The orange color filtrate was stripped off the solvent and precipitated from methanol to yield an orange-red colored powder. (0.040 g, 91%). ^{1}H NMR (400 MHz, $CDCl_3$, 25 °C): δ 7.41 (br), 7.11 (br), 6.25 (br), 4.04 (br), 3.45 (br), 2.06 (br), 1.85 (br), 1.54 (br), 1.35 (br), 0.89 (br).

Hybrid DCP (PS-Mo_6−PPV). In a two-neck flask were added deprotected DCP (0.030 g) and DCC (0.090 g, 0.436 mmol). The flask was degassed and backfilled with nitrogen. Hexamolybdate cluster, $[Mo_6O_{19}]^{2-} \cdot 2N(C_4H_9)_4^+$ (0.900 g, 0.659 mmol) dissolved in NMP (4 mL) was then added into the flask, and the reaction mixture was stirred at 100 °C for 12 h. The resulting dark red solution was cooled to room temperature, and the white solid precipitate (urea) was filtered off. The solvent was distilled off from the dark filtrate solution under vacuum, and the resulting concentrated solution was poured into hot acetonitrile to yield the crude hybrid DCP, which was further washed with hot acetonitrile to get rid of any remaining free cluster. The resulting hybrid DCP is a brownish red solid (0.035 g, 89%). ^{1}H NMR (400 MHz, $CDCl_3$, 25 °C): δ 7.48 (br), 7.15 (br), 6.71, (br), 4.05 (br), 3.42 (br), 1.85 (br), 1.66 (br), 1.54 (br), 1.30 (br), 1.05 (br), 0.89 (br).

Acknowledgment. This work is supported by the National Science Foundation (DMR 0804158).

Supporting Information Available: ^{13}C NMR spectra of monomers and polymers, additional optical spectra (absorption, fluorescence emission) of the polymers in both dilute solutions and as solid films, additional SEM and AFM images. This material is available free of charge via the Internet at http://pubs.acs.org.